VNU Journal of Science: Mathematics - Physics

Journal homepage: https://js.vnu.edu.vn/MaP

Photoluminescence Emission of Cu Doped ZnS Microstructures Synthesized by Thermal Evaporation

Nguyen Van Nghia[1,2,*], Nguyen Duy Hung[1]

[1]*Advanced Institute of Science and Technology (AIST), Hanoi University of Science and Technology, (HUST), 01 Dai Co Viet, Hanoi, Vietnam*

[2]*Thuy Loi University, 175 Tay Son, Dong Da, Hanoi, Vietnam*

Received 10 August 2017
Revised 05 September 2017; Accepted 15 November 2017

Abstract: Cu doped ZnS microstructures were prepared by the thermal evaporation method using ZnS powder and $CuCl_2.2H_2O$ powder as precusor materials. The microstructures was characterized by using X-ray diffraction (XRD) analysis. The XRD studies indicated that there are two phases (ZnS and ZnO) at the undoped sample, but most of the samples are only having wurtzite (hexagonal) phase of ZnS after doping. The photoluminescence emission and photoluminescence excitation of ZnS and Cu^{2+} doped ZnS microstructures have been studied. The photoluminescence excitation spectra of ZnS microstructures is presented around 374 nm. By doping of Cu^{2+} ion, the absorption wavelength is shifted towards the lower wavelength being an evidence for an increasing band gap. The emission spectrum of pure ZnS has a green emission band centred at around 520 nm. By doping Cu^{2+} ion, the peak of the green band in the luminescence spectra were transferred to 516 nm and appeared a strong blue peak at 440 nm. The reasons of these will be discussed in this paper.

Keywords: ZnS:Cu^{2+} microstructures, photoluminescence, thermal evaporation.

1. Introduction

Owning the largest band gap among II – VI semiconductor, zinc sulfide (ZnS), a direct transition semiconductor, is a famous material with diverse luminescence properties [1,2], Especially in doping the transition metals or rare earth elements [3–7]. Curently, it is used in many fields such as liquid crystal displays, light emitting diodes (LEDs), cathode ray tube (CRT) equipments and flat panel displays (FPDs) [8, 9].

*Corresponding author. Tel.: 84-984915472.
Email: nghiaaist@gmail.com

https//doi.org/ 10.25073/2588-1124/vnumap.4221

Recently, Mn-doped and Cu-doped ZnS structures have received much researchers' attention because the properties are closely related to the concentration of metal-doped [10–13]. The reason is that these metals can change the energy band and form luminescence centrals with different energy levels.

There are several approaches that have been conducted for the synthesis of pure ZnS and Cu-doped ZnS and controlled their morphology as soon as luminescence properties. In 2008, Datta et al have prepared Cu-doped ZnS nanorods by sovolthermal process. They exhibited that the wurtzite ZnS nanorods gradually phase transformed to cubic structure and photoluminescence intensities of UV and near IR bands changed with increasing the dopant concentration [14]. In 2012, Manuspiya et al have synthesized ZnS and metal (Mn, Cu)-doped-ZnS via wet chemical [15]. They found that ZnS, Mn-doped-ZnS and Cu-doped-ZnS generated blue, yellow and green color, respectively. Recently, in 2016, Shang et al also found that the optical emissions of ZnS nanostructures can be selectively modified through the control of Cu ion dose and subsequent heat treatment [16]. An increase of Cu dopant content will lead to an apparent red-shift of the intrinsic band-gap emission in the UV range and the broadening of defect-related emission in visible range.

In this research work, we present the synthesis of ZnS and Cu-doped ZnS microbelts by a thermal evaporation method. There are two peaks in the PL spectra at around 440 nm (blue) and 518 nm (green) at the same time when ZnS is doped by Cu with the rate of 10%mol. Different from ref. [14], phase of Cu-doped ZnS structures is wurtzite. The crystal structure, optical and surface morphological properties are all studied in detail.

2. Experiment

The Cu^{2+} doped ZnS microstructures were synthesized on Si/SiO_2 substrates by thermal vapor deposition in a conventional horizontal quartz tube furnace. A mixing of high-purity ZnS and $CuCl_2.2H_2O$ powders as the precursor materials were placed into an alumina boat and positioned at the center zone of the horizontal tube furnace. The ratio of $CuCl_2.4H_2O$ and ZnS powder is weighed with 0, 10, 50 and 100 mol%. Si/SiO_2 substrates with size of 0.5 x 0.5 cm were placed in the low temperature zone at about 15 cm downstream from the aluminum boat. A haft of the quartz tube containing the aluminum boat and Si/SiO_2 substrates was setup outside the tube furnace until the furnace was heated to deposition temperature. The quartz tube was pumped down to pressure of 1×10^{-3} Torr and heated to 600 ^oC, then the high-purity argon was introduced into the tube and the mechanical rotary pump was turn off. The flow rates of Ar were controlled by a mass flow meter at 120 sccm. The temperature of the furnace was raised continually to growth temperature at a ramping rate of 10 ^oC/min. The deposition temperature was set up at 1100 ^oC. When temperature of the furnace increased to deposition temperature, the part of quartz tube containing the aluminum boat and Si/SiO_2 substrates was pushed into the furnace to grow microbelts. During synthesis the furnace temperature was maintained at growth temperature for 30 min, after that the furnace was allowed to cool naturally to room temperature.

The morphology was examined by a field emission scanning electron microscopy (FESEM, JSM-7600F, Jeol). The composition was determined by the energy dispersive x-ray spectroscopy (EDX, Oxford Instruments X-Max 50) attached to the FESEM. The phase structure, crystallinity and preferred orientation of as-synthesized microstructures were characterized by an X-ray diffraction (XRD) (X-ray Siemens D5000) using Cu Kα radiation (λ=1.5406 Å) operated at 40 mA tube current. The XRD patterns were collected in the range of $20\ ^\circ \leq 2\theta \leq 70\ ^\circ$ with a step of 0.05 ° and collection time for each data point was set at 4 seconds. The photoluminescence spectra (PL) and

photoluminescence excitation spectra (PLE) were recorded on Horiba Jobin–Yvon Nano-Log spectrometers using a Xenon lamp (450 W) as an excitation source.

3. Results and discussion

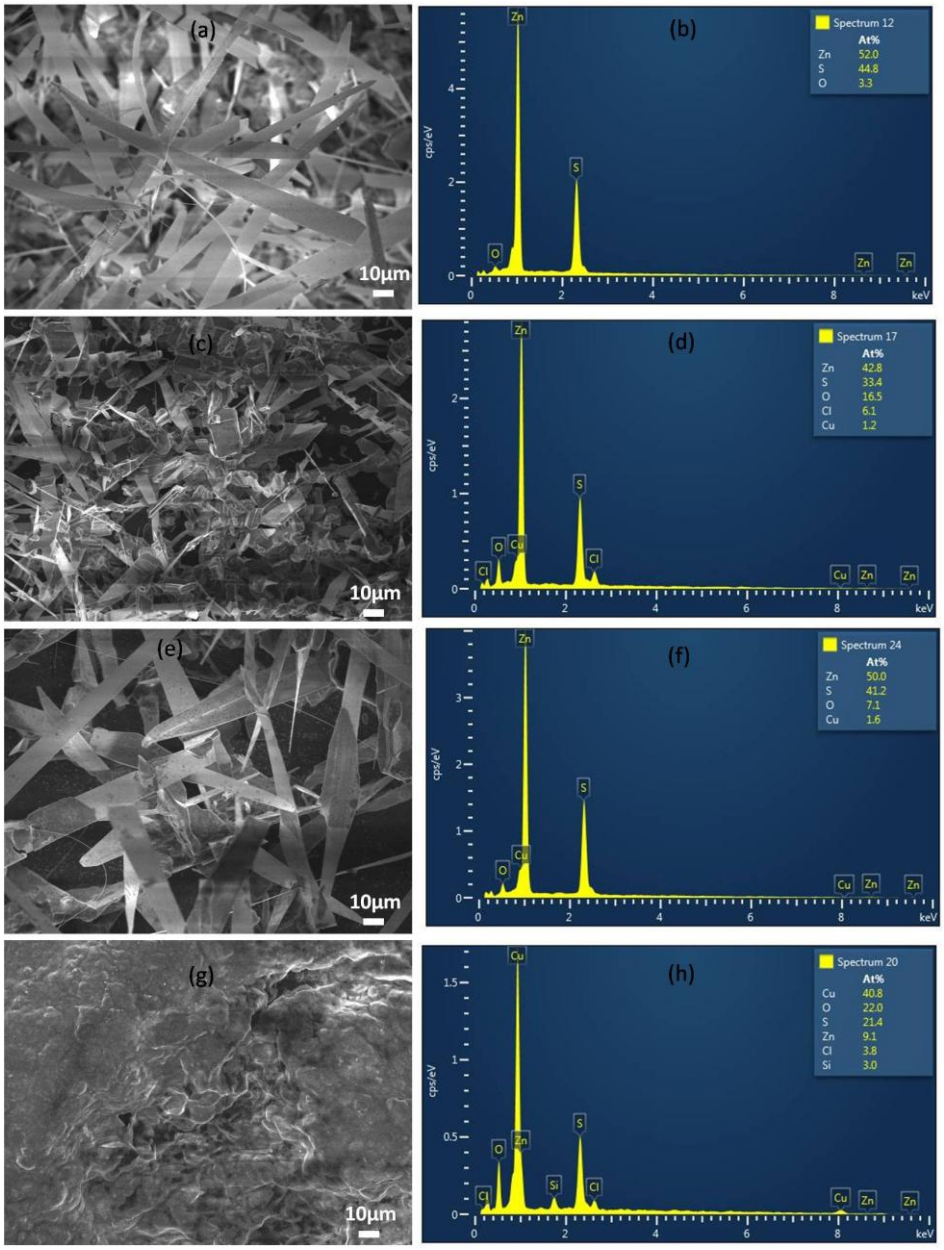

Figure 1. FESEM images and EDS of ZnS microstructures rate of Cu and ZnS is 0 mol% (a,b), 10 mol% (c,d), 50 mol% (e,f) and 100 mol% (g,h).

To study the morphology of the structures, FESEM were employed. Fig. 1 shows a series of FESEM images of the structures grown on Si/SiO_2 substrates. A typical FESEM image shows that undoped ZnS microbelts is high density with several microns to about ten microns in widths and several tens to more than one hundred of microns in lengths (Fig. 1a). These microbelts are quite smooth, and their orientations are random. Making clusters and structures as microsheets is the trend that can be seen clearly for Cu-doped ZnS with 10%mol. When ZnS is doped with Cu at 50%mol, the microsheets become larger than the undoped microbelts and the density of them is low. However, for Cu-doped ZnS with 100%mol, all of the material turned into cluster and no microbelts or microsheets were seen. The corresponding EDS spectra reveal that the undoped microbelts mainly contain Zn, S and O elements and the atom ratio of undoped ZnS is 53.0, 44.8 and 3.3 at%. The origin of O atom may come from reaction between ZnS and O_2 existing in furnace tube which was not pumped to low enough pressure or origin from ZnS powder (precusor material). By doping Cu^{2+} with 10%mol, the Cl and Cu components appear with atom ratio of 6.1 and 1.2%, respectively. At 50%mol of Cu content, the atom ratio of Cu in the microsheets go up to 1.6%. However, the Cu component increases rapidly to 40.8%, and the Si component appears with atom ratio of 3.0% at the doping content of 100%mol. The Cl composition maybe come from $CuCl_2.2H_2O$ precursor, while Si composition is attributed to Si/SiO_2 substrate due to thin material located in it.

XRD measurement was performed in order to determine the crystalline phase of the microstructures. It is clear from Figure 2 that all of microstructures doped or undoped Cu are matched to the structure of wurtzite (JCPDS 05-0492). In detail, the XRD pattern of the microbelts without doping shows a peak at 27.87^o corresponding to (111) plane of cubic phase (JCPDS card no. 05-0566) while all of other peaks are wurtzite phase of ZnS. When the precursor material is mixed with 10 mol% of Cu, the peak of cubic phase disappears and the intensity of all peaks corresponding to wurzite phase increases. However, when the concentration of Cu goes up to 40 mol%, the intensity of all peaks decreases and becomes very weak at 100 mol%. This proves that crystal quality of ZnS is changed through doping with Cu^{2+} ions.

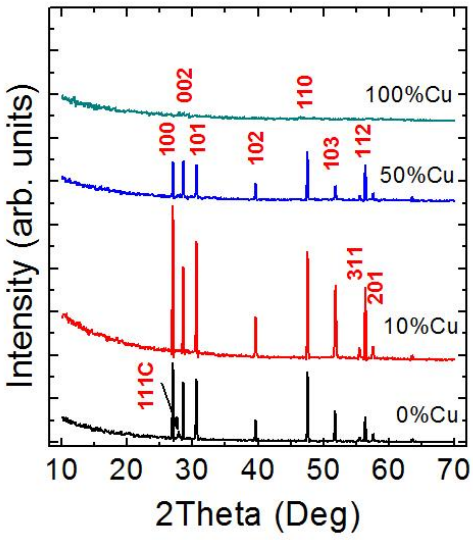

Figure 2. XRD pattern of Cu doped ZnS microstructures grown on Si/SiO2 substrates.

In order to investigate the optical properties of the samples, the PL spectra of ZnS and ZnS:Cu^{2+} microstructures were measured at room temperature using a 280-nm excitation wavelength (Figure 3). For the undoped sample, PL spectrum shows a emission band in visible region at around 520 nm. The study groups of Zhang and Changxin Guo have reported that the green emission at 520 nm from ZnS nanowires and nanobelts originates from Au impurity [17]. In 2016, the other group found that the emergence of the green emission is directly related to the formation of the ZnO layer and the imperfect surface/interface between the newly formed ZnO and the ZnS backbone [18]. In our situation, from EDS analysic and XRD pattern, no phase relative Au was seen from the microbelts, so this green peak may come from radiative centers of ZnS and ZnO [13, 19, 20]. The ZnS:Cu microsheets show more peaks, at 440 nm and 518 nm for 10 mol% being different from undoped sample. At higher content of Cu with 50 mol%, there are only one blue peak at around 443 nm with very high intensity. However, at the sample doped with 100%mol of Cu, the intensity of blue emission band went down significantly and there are two new peaks at 346 nm and 510 nm beside a blue peak at 440 nm. From the PL spectra and Refs [21–23], the blue emission bands are attributed to the surface defects such as sulfur vacancy or sulfur interstitial lattice defects. Meanwhile, the green emissions may be assigned to the surface defects such as oxygen vacancies [13].

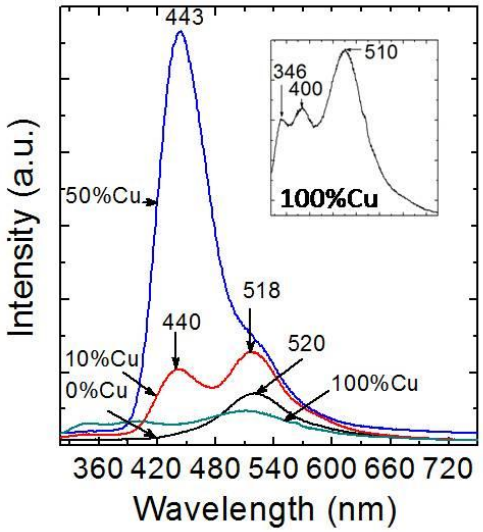

Figure 3. PL spectra of undoped and Cu^{2+} doped ZnS microstructures.

In order to further investigation about the effect of Cu on the radiative centers of ZnS microbelts, the PLE spectra of the products which monitored at the emission wavelength of 440 nm are shown in Fig. 4. At undoped sample, the spectra show that the microbelts are absorbed strongly at around 374 nm which are corresponded with the bandgap of ZnS, ZnO or ZnOS [24]. When the contents of Cu are 10% and 50% mol, the absorption edge transfers to short wavelength at around 362 nm and 359 nm, respectively. At the same time, there are some very strong peaks at around 332 nm and 340 nm corresponding to the fundamental absorption of ZnS [25]. The absorption related to the band to band transition of ZnO or ZnOS reduces from 374 nm to 359 nm when the content of Cu^{2+} increases. This result shows that the emission of the radiative centers of ZnS microstructures are modified by Cu^{2+}

ions and the emission at blue emission is originated from defects of Zn and S in the ZnS crystal. However, at content of Cu is 100%mol, the absorption peak comes back at around 369 nm. The reason may be that at very high content, Cu^{2+} ions have a trend making clusters, so the emission centers return to ZnS host.

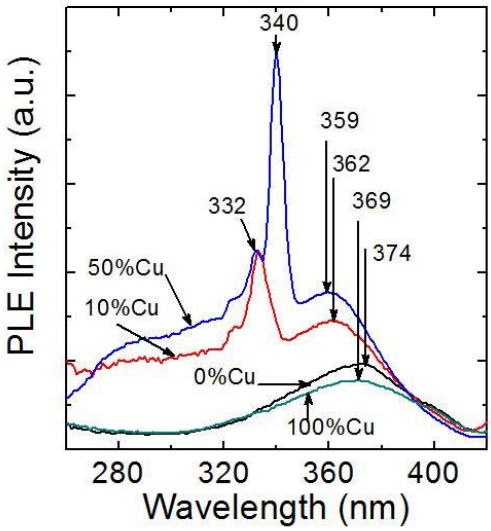

Figure 4. PLE spectra of undoped and Cu^{2+} doped ZnS microstructures.

4. Conclusion

The undoped and Cu doped ZnS microstructures on Si/SiO_2 substrates have been successfully synthesized by a thermal evaporation method. The undoped ZnS microbelts shows a broad band emission at visible region at around 520 nm which related to radiative centers of ZnS and ZnO. By doping Cu with various concentration, the emission band of radiative centers related to S and O in the ZnS microbelts separated into blue and green emission, respectively. The green emission band dominates as the doped Cu concentration is high enough and then to be quenched at the doping of 100%mol. Thus, the emission of radiative centers of ZnS can be controlled by Cu concentration doped into ZnS microstructures.

References

[1] H. Hiramatsu, H. Ohta, M. Hirano, and H. Hosono, Heteroepitaxial growth of single-phase zinc blende ZnS films on transparent substrates by pulsed laser deposition under H2S atmosphere, Solid State Commun., 124 (2002) 411.

[2] K. Ichino, K. Ueyama, H. Kariya, N. Suzuki, M. Kitagawa, and H. Kobayashi, Photoluminescence study of ZnS / ZnMgS single quantum wells, Appl. Phys. Lett., 74 (1999) 3486.

[3] W. Jian, J. Zhuang, W. Yang, and Y. Bai, Improved photoluminescence of ZnS:Mn nanocrystals by microwave assisted growth of ZnS shell, J. Lumin., 126 (2007) 735.

[4] W. Q. Peng, G. W. Cong, S. C. Qu, and Z. G. Wang, Synthesis and photoluminescence of ZnS:Cu nanoparticles, Opt. Mater. (Amst)., 29 (2006) 313.

[5] L. Wanjari, D. P. Bisen, N. Brahme, I. Prasad Sahu, and R. Sharma, Effect of capping agent concentration on thermoluminescence and photoluminescence of copper-doped zinc sulfide nanoparticles, Luminescence, 30 (2015) 655.

[6] R. K. Tamrakar, UV-irradiated thermoluminescence studies of bulk CdS with trap parameter, Res. Chem. Intermed., 41 (2015) 43.

[7] D. Li, B. L. Clark, D. A. Keszler, P. Keir, and J. F. Wager, Color control in sulfide phosphors: Turning up the light for electroluminescent displays, Chem. Mater., 12 (2000) 268.

[8] J. Bang, B. Abrams, B. Wagner, and P. H. Holloway, Effects of coatings on temporal cathodoluminescence quenching in ZnS:Ag,Cl phosphors, J. Appl. Phys., 95 (2004) 7873.

[9] P. D. Rack and P. H. Holloway, The structure, device physics, and material properties of thin film electroluminescent displays, Mater. Sci. Eng. R Reports, 21 (1998) 171.

[10] L. Luo, H. Chen, L. Zhang, K. Xu, and Y. Lv, A cataluminescence gas sensor for carbon tetrachloride based on nanosized ZnS, Anal. Chim. Acta, 635 (2009) 183.

[11] B. Dong, L. Cao, G. Su, W. Liu, H. Qu, and D. Jiang, Synthesis and characterization of the water-soluble silica-coated ZnS:Mn nanoparticles as fluorescent sensor for Cu2+ ions, J. Colloid Interface Sci., 339 (2009) 78.

[12] N. Üzar, S. Okur, and M. Ç. Arikan, Investigation of humidity sensing properties of ZnS nanowires synthesized by vapor liquid solid (VLS) technique, Sensors Actuators, A Phys., 167 (2011) 188.

[13] H. Tang, B. J. Kwon, J. Kim, and J. Y. Park, Growth modes of ZnS nanostructures on the different substrates, J. Phys. Chem. C, 114 (2010) 21366.

[14] A. Datta, S. K. Panda, and S. Chaudhuri, Phase transformation and optical properties of Cu-doped ZnS nanorods, J. Solid State Chem., 181 (2008) 2332.

[15] S. Ummartyotin, N. Bunnak, J. Juntaro, M. Sain, and H. Manuspiya, Synthesis and luminescence properties of ZnS and metal (Mn, Cu)-doped-ZnS ceramic powder, Solid State Sci., 14 (2012) 299.

[16] L. Y. Shang, D. Zhang, and B. Y. Liu, Influence of Cu ion implantation on the microstructure and cathodoluminescence of ZnS nanostructures, Phys. E Low-Dimensional Syst. Nanostructures, 81 (2016) 315.

[17] J. Hu, G. Wang, C. Guo, D. Li, L. Zhang, and J. Zhao, Au-catalyst growth and photoluminescence of zinc-blende and wurtzite ZnS nanobelts via chemical vapor deposition, J. Lumin., 122–123 (2007) 172.

[18] D. Q. Trung, N. Tu, N. D. Hung, and P. T. Huy, Probing the origin of green emission in 1D ZnS nanostructures, J. Lumin., 169 (2016) 165.

[19] T. Mitsui, N. Yamamoto, T. Tadokoro, and S. Ohta, Cathodoluminescence image of defects and luminescence centers in ZnS/GaAs (100), J. Appl. Phys., 80 (1996) 6972.

[20] G. H. Yue et al., Hydrothermal synthesis of single-crystal ZnS nanowires, Appl. Phys. A Mater. Sci. Process., 84 (2006) 409.

[21] S. Wageh, Z. S. Ling, and X. Xu-Rong, Growth and optical properties of colloidal ZnS nanoparticles, J. Cryst. Growth, 255 (2003) 332.

[22] A. Goudarzi et al., Low-Temperature Growth of Nanocrystalline Mn-Doped ZnS Thin Films Prepared by Chemical Bath Deposition and Optical Properties, Chem. Mater., 21 (2009) 2375.

[23] W. W. G. Becker and A. A. J. Bard, Photoluminescence and photoinduced oxygen adsorption of colloidal zinc sulfide dispersions, J. Phys. Chem., 78712 (1983) 4888.

[24] N. Xuan, Fabrication and Photoluminescence Properties of ZnS Nanoribbons and Nanowires, 52 (2008) 1530.

[25] Y. Y. Bacherikov et al., Structural and optical properties of ZnS:Mn micro-powders, synthesized from the charge with a different Zn/S ratio, J. Mater. Sci. Mater. Electron., 28 (2017) 8569.